MODELING OF COHERENT SYNCHROTRON RADIATION USING A DIRECT NUMERICAL SOLUTION OF MAXWELL'S EQUATIONS*

A. Novokhatski#, SLAC National Accelerator Laboratory,
Menlo Park, CA 94025, USA

Abstract

We present and discuss the properties of coherent electromagnetic fields of a very short, ultra-relativistic bunch, which travels in a rectangular vacuum chamber under the influence of a bending force of a magnet. The analysis is based on the results of a direct numerical solution of Maxwell's equations together with Newton's equations. We use a new dispersion-free time-domain algorithm which employs a more efficient use of finite element mesh techniques and hence produces self-consistent and stable solutions for very short bunches. We investigate the fine structure of the CSR fields. We also discuss coherent edge radiation. We present a clear picture of the field using the electric field lines constructed from the numerical solutions. This approach should be useful in the study of existing and future concepts of particle accelerators and ultrafast coherent light sources, where high peak currents and very short bunches are envisioned.

INTRODUCTION

The coherent synchrotron radiation (CSR) fields have a strong action on the beam dynamics of very short bunches, which are moving in the bends of all kinds of magnetic elements. They are responsible for additional energy loss and energy spread; micro bunching and beam emittance growth. These fields may bound the efficiency of damping rings, electron-positron colliders and ultrafast coherent light sources, where high peak currents and very short bunches are envisioned. This is relevant to most high-brightness beam applications. On the other hand, these fields together with transition radiation fields can be used for beam diagnostics or even as a powerful source of THz radiation.

A history of the study of CSR and a good collection of references can be found in [1]. Electromagnetic theory suggests several methods on how to numerically calculate CSR fields. The most popular method is to use Lienard-Wiechert potentials. Another approach is to numerically solve the approximate equations, which are a Schrodinger type equation. Some numerical algorithms and codes are described in [2]. We suggest that a direct solution of Maxwell's equations together with Newton's equations can describe the detailed structure of the CSR fields [3].

Modeling ultrafast phenomena requires a special algorithm for solving the electromagnetic equations. This algorithm must be free of frequency dispersion which means that all propagating waves must have their natural phase velocity, completely independent of the simulation parameters like mesh size or time step. We suggest an implicit algorithm which does not have stability issues and employs a more efficient use of finite element mesh techniques. This method can produce self-consistent stable solutions for very short bunches. We have already used this same approach long ago for wake field calculations. An implicit, dispersion-free time-domain algorithm was used in the computer code designed in 1976 for wake field dynamics studies at the Novosibirsk Electron-Positron Linear Collider VLEPP [4]. The algorithm details can be found in [5].

*Work supported by Department of Energy contract DE–AC03–76SF00515.
#novo@slac.stanford.edu

ELECTROMAGNETIC CSR SIMULATION

We may suggest that a direct solution of Maxwell's equations together with Newton's equations can describe the detailed structure of the CSR fields, the fields generated by an ultra-relativistic bunch of charged particles moving in a metal vacuum chamber inside a bending magnet. Electromagnetic components **E, B** must satisfy the equations

$$\frac{1}{c}\frac{\partial}{\partial t}\mathbf{E} = \nabla\times\mathbf{B} - \frac{4\pi}{c}\mathbf{j}_b \qquad \nabla\cdot\mathbf{E} = 4\pi\rho_b \qquad \mathbf{E}_{wall}\times\mathbf{n} = 0$$

$$\frac{1}{c}\frac{\partial}{\partial t}\mathbf{B} = -\nabla\times\mathbf{E} \qquad \nabla\cdot\mathbf{B} = 0 \qquad \mathbf{B}_{wall}\cdot\mathbf{n} = 0$$

A charge density and a charge current must satisfy a continuity equation

$$\rho_b = \sum_k \rho_k(\mathbf{x}) \qquad \boldsymbol{j}_b = \sum_k \rho_k(\mathbf{x})\mathbf{v}_k \qquad \nabla\cdot\mathbf{j}_b + \frac{1}{c}\frac{d}{dt}\rho_b = 0$$

A Newton force includes electromagnetic components and a bending magnetic field

$$\frac{d}{dt}\mathbf{p}_k = e\mathbf{E} + \frac{\mathbf{v}_k}{c}\times e\left(\mathbf{B} + \mathbf{B}_{bend}\right) \qquad \mathbf{p}_k = m\mathbf{v}_k \Big/ \sqrt{1-\frac{v_k^2}{c^2}}$$

There are a lot of finite-difference schemes, which numerically solve Maxwell's equations since the first one was published in 1966 [6]. Most of them are so-called ''explicit'' schemes, which means that the value of the field at the new time step is calculated only by the field values from the previous time step. Stability conditions for these schemes do not allow a time step to be greater than or equal to a space (mesh) step. This limitation brings an additional troublesome effect for wavelengths that are comparable to a mesh step. We state that this effect works like a frequency dispersion media, which is ''hidden'' in the finite-difference equation.

ISBN 978-3-95450-116-8

Dispersion of the Explicit Schemes

Let's check the explicit scheme for the two-dimensional case. When the field components satisfy the equation:

$$\frac{\partial^2\Phi}{c^2\partial t^2}=\frac{\partial^2\Phi}{\partial z^2}+\frac{\partial^2\Phi}{\partial x^2}$$

likewise the explicit scheme will be

$$\Phi^{n+1}-2\Phi^n+\Phi^{n-1}=\left(\frac{c\Delta t}{\Delta z}\right)^2\Delta_z^2\Phi^n+\left(\frac{c\Delta t}{\Delta x}\right)^2\Delta_x^2\Phi^n$$

The stability condition easily comes from the Fourier analyses $\Phi_k^n \sim e^{i\omega t+i\beta z+i\alpha x}$ and takes the form:

$$\sin^2\frac{\omega\Delta t}{2}=\left(\frac{c\Delta t}{\Delta z}\right)^2\times\sin^2\frac{\beta\Delta z}{2}+\left(\frac{c\Delta t}{\Delta x}\right)^2\times\sin^2\frac{\alpha\Delta x}{2}$$

For stability reasons we need the frequency ω to be real. This happens when the right part is less than one. To have stability for any longitudinal wave vector β and transverse wave vector α we need the following condition to be fulfilled

$$\left(\frac{c\Delta t}{\Delta z}\right)^2+\left(\frac{c\Delta t}{\Delta x}\right)^2\le 1 \quad \text{for } \Delta x=\Delta z \quad c\Delta t\le\frac{1}{\sqrt{2}}\Delta z$$

Now let's check the plane waves in free space. Without boundaries the plane waves must propagate at the speed of light. However the solution of the finite-difference equation shows that the propagation velocity depends upon the frequency.

$$V_{wave}=\frac{\omega}{\beta}=c\frac{2}{\beta c\Delta t}\times\arcsin\left(\frac{c\Delta t}{\Delta z}\sin\frac{\beta\Delta z}{2}\right)$$

This means that finite-difference equations contain something like a "hidden" dispersion media, which reveals itself at a wavelength comparable to the mesh size. A plot of propagation velocity as a function of frequency for different ratios of mesh steps to time steps is shown in Fig. 1.

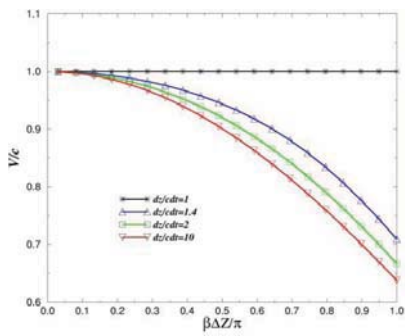

Figure 1: Propagation velocity of a plane wave in free space as a function of frequency for different ratios of mesh steps to time steps.

This numerical dispersion disappears only when the time step becomes equal to the mesh step, but in this case the scheme is unstable. The effect of the numerical dispersion may be very dangerous; it can greatly disturb the result. It may develop a strong diffusion of an initially smooth field distribution and reveal high frequency oscillations. Fig. 2 shows snap shots of a short wave bucket propagating in free space. This is the result of using the explicit scheme for the case when the length of a bucket is equal to two mesh sizes. We can see that a wave bucket has distortion, modulation and diffusion: everything that comes from a dispersion media. The numerical dispersion distorts the bucket shape. If we want to have a better result using the explicit scheme we need to decrease the mesh size least five times. In the wake field simulations this effect leads to an unphysical result like "self-acceleration" of a bunch head, which violates energy conservation. The explicit scheme ends up being not very good at calculating the wake fields of very short bunches.

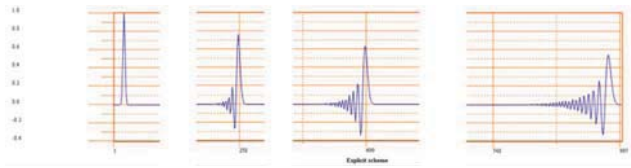

Figure 2: Snap shots of a propagating short wave bucket, calculated by an explicit scheme.

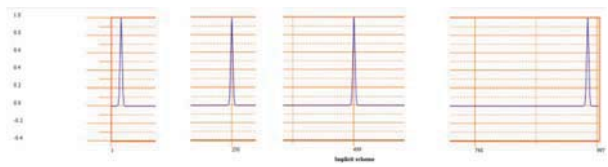

Figure 3: Snap shots of a propagating short wave bucket, calculated by an implicit scheme.

Implicit Scheme

As we stated before there will be no numerical dispersion if the time is equal to a mesh step. We can fulfil this condition by using the stable implicit scheme. In the implicit scheme for the calculation of the space derivatives we assume that the field at some time can be approximated by the average value of the field at a previous and a new time step. Of course the implicit algorithm is more complicated as it requires the solution of a system of equations. However, as we are interested in the waves that are propagating in the longitudinal direction we really only need a "partially" implicit scheme, which for our equation is the following:

$$\Phi^{n+1}-2\Phi^n+\Phi^{n-1}=\left(\frac{c\Delta t}{\Delta z}\right)^2\Delta_z^2\Phi^n+\left(\frac{c\Delta t}{\Delta x}\right)^2\Delta_x^2\frac{1}{2}\left(\Phi^{n+1}+\Phi^{n-1}\right)$$

The dispersion relation for this scheme is:

$$\sin^2\frac{\omega\Delta t}{2}=\frac{\left(\frac{c\Delta t}{\Delta z}\right)^2\sin^2\beta\frac{\Delta z}{2}+\left(\frac{c\Delta t}{\Delta x}\right)^2\sin^2\alpha\frac{\Delta x}{2}}{1+2\left(\frac{c\Delta t}{\Delta x}\right)^2\sin^2\alpha\frac{\Delta x}{2}}$$

This equation shows that this scheme is stable in the case of equal mesh and time step $c\Delta t=\Delta z$. Fig. 3 demonstrates the effectiveness of this scheme. Now a wave bucket keeps the same shape.

MAIN STRATEGY OF THE METHOD

The main strategy of our method is to use an implicit algorithm which does not have stability issues and employs a more efficient use of finite element mesh techniques. The scheme may have dispersion in the transverse

ISBN 978-3-95450-116-8

direction. However, electromagnetic fields, which interact with a beam, propagate in the vacuum chamber at small angles, so the effect of dispersion in the transverse direction is less important than dispersion in the longitudinal direction. To employ the implicit scheme we transform Maxwell's equations to second order equations.

We also use the Fourier series expansion in the vertical direction. This approach allows to make 3D simulations on the assumption that there is no vertical motion of the beam and the vertical size of a beam chamber is constant. We also assume that the conductivity of the wall of the beam chamber is infinite.

To decrease the amount of needed memory we use a traveling mesh. This is very important for simulations of real devices, like a bunch compressor where the distance between bends is tens of meters but the bunch length is of a micron size. Our mesh will move with the speed of light and we can definitely assume that the electromagnetic field in front of the bunch is zero; even if the bunch motion is not straight. Because a time delay or a longitudinal position delay due to the rotation in a bending magnet is very small, we really do not need more mesh space for the bunch. In our case a traveling mesh does not change the accuracy of the scheme or any conditions of stability.

To simulate the real shape of a non-monochromatic bunch moving under the action of the electromagnetic fields including vertical magnetic fields of bending magnets, we will use an ensemble of particles. We will track each particle and average the current (particle velocities) over the mesh. The charge density distribution will be integrated using the continuity equation for charge and current. This will help to smooth out errors of particle transitions from one cell to another. Later we will show a charge distribution of a bunch rotated by the vertical magnetic field. We also assume that initially a bunch has a Gaussian distribution in all directions and is travelling with a speed very close to the speed of light. In this case we can easily calculate the initial distribution of the electromagnetic field of a bunch equal to the field of a bunch traveling in infinite metallic beam chamber. More details of this method can be found in [7-8].

CSR FIELD DYNAMICS

Radiation in a Bend

Let us first try to understand how a bunch field remakes itself when a bunch is rotated in a magnetic field. We have calculated the electromagnetic field of a three dimensional Gaussian bunch that is initially moving along the vacuum chamber very close to the speed of light. At some point the bunch enters a vertical magnetic field of a bend. What happens after can be seen at Fig. 4, where snapshots of the electric field line distributions are shown at different time moments. In these plots the white boxes with the red arrows show a bunch contour and a bunch velocity direction. Before entering a bend the bunch has only a transverse field, which can be seen as a set of vertical lines. A new field that is generated in a bend is a set of ovals, which increase in size with a time. We can outline two time periods of the field formation. The first period is when a bunch is still inside the region of its initial transverse field. The first two plots in Fig. 4 are related to this first period. The second period starts when the bunch is delayed so much that it is out of the region of the initial transverse field. The bunch is delayed because the velocity vector rotates and the longitudinal component becomes smaller and smaller than the speed of light, however field lines that are not very far away "don't know" about this change and continue to propagate at the speed of light. The last plot in Fig. 4 shows this situation. We may consider these fields to be the fields of the edge radiation in a bend.

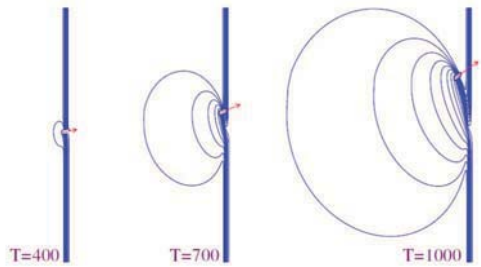

Figure 4: Snapshots of electric field lines of a bunch, which is moving in a magnetic field. White boxes show the bunch contour. Red arrows show the directions of the bunch velocity.

A more detailed picture of the field lines is shown in Fig. 5, where we also show the directions of the electric field lines by green arrows. If one examines this picture he can see that the upper field lines take the position of the lower lines and a part of the lower field lines take the position of the upper lines. However at the far ends the transverse field lines continue traveling in the same initial direction.

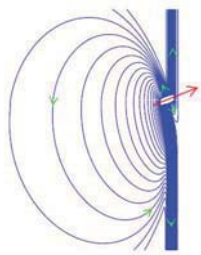

Figure 5: Detailed structure of the field pattern.

We can easily to explain such behavior if we present this field as a sum of two fields: $E = E_{db} + E_{in}$. The first part is the field of a dipole, which consists of two oppositely charged bunches. One bunch, which has a positive charge is the "real" one. This bunch is rotated in the magnetic field while the other bunch is a "virtual" one, which has an opposite charge and travels straight in the initial bunch direction. The second field $\mathbf{E}_{in}$ is the field of another "virtual", but positively charged bunch, which travels straight along the initial bunch direction. Naturally the virtual bunches together sum to zero. When we decompose the charges we decompose the fields and the

ISBN 978-3-95450-116-8

very complicated structure of the radiation field becomes simple. The decomposition of the field is shown in Fig. 6.

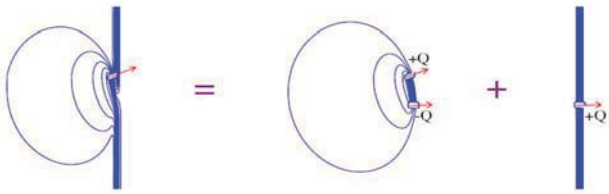

Figure 6: Decomposition of the field of a bunch moving in a magnetic field (left plot) into two fields: a field of a dipole (middle plot) and a field of a bunch moving straight in the initial direction (right plot). Red arrows show the directions of the bunch velocities.

The interaction of the bunch with the dipole field continues for a longer time. Fig. 7 shows the absolute value of the electric field on the horizontal plane in the vertical center of the vacuum chamber in consecutive time steps. The white oval shows the real bunch contour. When a dipole is created an electric field appears between a real bunch and a virtual bunch. This field increases in value and reaches a maximum when the bunches are completely separated and then decreases as the bunches move apart leaving the fields only around the bunches. The bunch acquires an energy loss while interacting with the electric dipole field.

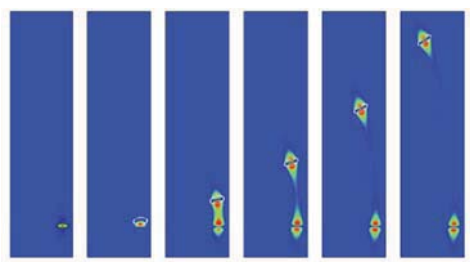

Figure 7: Absolute value of the electric field of a dipole.

Continuing the study of the radiation process we investigate the dense set of field lines in Fig. 5, or the fine structure of the field in front of a bunch. This region is common with classical synchrotron radiation. The characteristic wavelength of the synchrotron radiation or an equivalent value of the bunch length for this relativistic factor is

$$\sigma_{s.r.} \approx \frac{R}{\gamma^3}$$

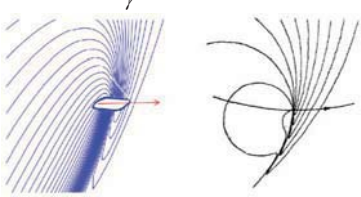

Figure 8: Fine structure of the field pattern in front of a bunch. The left plot shows field lines near a bunch. The right plot presents a picture from reference [9].

We chose reference [9], as it supplies a picture of the field lines of a particle moving in a circle with a relativistic factor of γ=6. The equivalent value of the bunch length for this relativistic factor is very close to our bunch length. Fig. 8 shows this finite structure together with a plot from [9]. We can state that the region before a bunch is very close for both cases.

Fields Acting Inside a Bunch

In order to study the fields acting on the particles inside the bunch we calculate the distribution of a collinear force $E_{||}$ and a transverse force $E_{\perp}$ as projections to the bunch velocity

$$\mathbf{F}_{||} = \mathbf{J}_b \cdot \mathbf{E} \quad \mathbf{F}_{\perp} = \left[\mathbf{J}_b \times \mathbf{E}\right]_x$$

We have found some very exciting fine structure from this force acting on the particles in the bunch. Fig. 9 shows a distribution of forces in the horizontal plane in the vertical center of the vacuum chamber at three time moments. The left three vertical plots in Fig. 9 show a bunch charge distribution. The starting plots at each set are at the bottom when the bunch just enters the magnetic field. The red arrows show the direction of the bunch velocity. The middle three vertical plots show a transverse force. Again, the red arrow shows the direction of the force. The transverse force is the well-known space-charge force, which probably is compensated by a magnetic force in the ultra-relativistic case. The right three vertical plots show the collinear force, which is responsible for an energy gain or an energy loss. The red color corresponds to acceleration and energy gain and the blue color corresponds to deceleration or energy loss. The red arrows are collinear or anti-collinear with the bunch velocity.

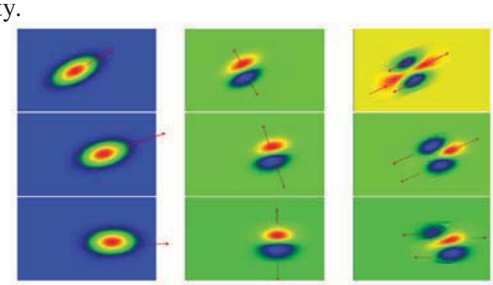

Figure 9: Bunch charge distributions, transverse forces and collinear forces on the horizontal plane in the vertical center of the vacuum chamber at three time moments.

We see here that the forces on the bunch are very complicated. The particles, which are in the center of the bunch, in front of the bunch and at the end are accelerated, whereas the particles at the boundaries are decelerating. This means that a bunch gets an additional energy spread in the transverse direction. The total effect is deceleration and the bunch loses energy. The asymmetry of the longitudinal fields can also be seen in Fig. 5, which shows the electric field line distributions. The bunch shape deformation due to the difference in the angular velocity along the radial position is usually small and can be seen only after some time; however the ultra-small beam emittance can be effected.

The integrated energy loss along the transverse direction as a function of the longitudinal coordinate is shown in Fig. 10 together with a bunch longitudinal

ISBN 978-3-95450-116-8

distribution. One can see that the head of the bunch and the tail are accelerated, when the rest of the bunch is decelerated. The shape of the energy loss distribution is compared with the analytical 1-D model [10] (green dashed line). We obtain a better agreement with the shape of the energy loss distribution for a larger bending radius and smaller bunch length. This comparison is shown at the right plot of Fig. 10. The transverse energy spread is smaller for a larger bending radius.

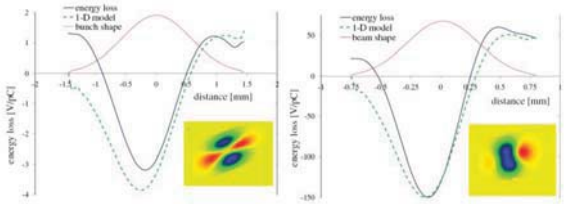

Figure10: Integrated energy loss along the transverse direction as a function of the longitudinal coordinate for two values of bending radius.

Coherent Edge Radiation

As we mentioned above, an ultra-relativistic bunch and CSR fields are moving together and interact for a long time. However one can see a field, which propagates straight ahead from the initial beam horizontal position. This field can be seen very well when the bunch gets a large horizontal displacement. Fig. 11 shows the distribution of the magnetic field on the horizontal plane in the vertical middle of the vacuum chamber. The large peak corresponds to the bunch field. A red arrow shows the initial bunch X-position and the direction of the bunch velocity. A blue arrow shows the direction of the bunch velocity at this time.

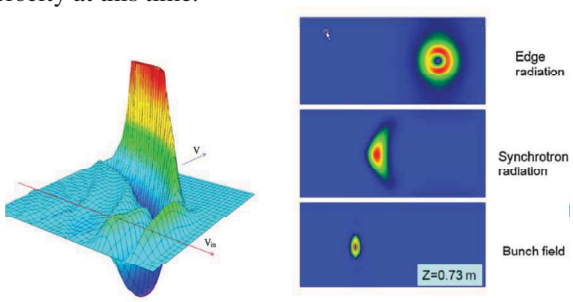

Figure11: Coherent edge radiation.

The right plot shows images of the coherent radiation in the form of transverse magnetic field distributions on the vertical planes of the vacuum chamber. At first we see an image of edge radiation, then the image of synchrotron radiation and finally a bunch field image. The calculated images of the coherent edge radiation look very similar to the images, which we have seen on the YAG screen after the dump magnets, which bend the beam down at LCLS.

Fields in the Beam Chamber of an Accelerator

As we mentioned before, the metal walls of a vacuum chamber of an accelerator change the distribution of the radiation fields, but the self-electromagnetic field of a bunch is also modified by the chamber geometry. This field is much stronger than the radiation fields. Fig. 12 shows the vertical electric field component inside the chamber when a bunch has left a magnet. The shape of the chamber follows the bunch trajectory. To see the radiation fields we need to magnify the amplitude 1000 times. When a bunch changes position in a chamber, its electromagnetic field also changes and the bunch must react back: loosing and then gaining the kinetic energy. In some cases this effect can be a much stronger radiation loss.

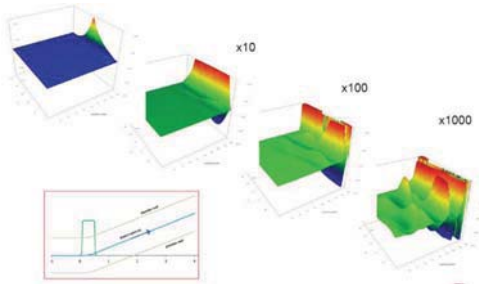

Figure 12: Magnified vertical component of the electric field of a bunch moving in a vacuum chamber after having been bent by a magnet.

CONCLUSIONS

We have found that there is much a more interesting and detailed structure to the CSR fields, which have not been described by any previous study. A very important result is discovering the structure of the complicated collinear forces. A bunch will get an additional energy spread in the transverse direction from the collinear force. This immediately leads to emittance growth and decoherence that could limit FEL lasing for very short bunches. We will continue to study this effect.

ACKNOWLEDGMENTS

The author would like to thank Mike Sullivan for help and valuable comments, Franz-Josef Decker, Paul J. Emma and Yunhai Cai for support and interest in this work and physicists of the Beam Physics Department for useful discussions.

REFERENCES

[1] J. B. Murphy, ICFA B. D. Newsletter, No.35 (2004).
[2] G. Bassi et al., Nuc. Instrum. Methods Phys. Res. A, 557, pp. 189-204 (2006).
[3] A. Novokhatski, M. Sullivan, IPAC'2010, Kyoto, May 2010.
[4] V. Balakin et al., Proc. of the All Union Accelerator Conference, Dubna, 1978, page 143. Translated to English: SLAC TRANS-188, November 1978.
[5] A. Novokhatski, SLAC-PUB-11251, May 2005.
[6] Yee KS. IEEE Transactions on Antennas and Propagation 1966; 14(3):302-307.
[7] A. Novokhatski, PAC'2011, New York, March 2011
[8] A. Novokhatski, Phys.Rev.STAB, 14 (2011) 060707.
[9] S. G. Arutyunyan, Sov. Phys. Usp. 29, 1053-1057 (1986)
[10] Ya. S. Derbenev et al., TESLA FEL-Report 1995-05 (1995)

ISBN 978-3-95450-116-8